

Preterm birth leads to impaired rich-club organization and fronto-paralimbic/limbic structural connectivity in newborns

Joana Sa de Almeida^a, Djalel-Eddine Meskaldji^{a,b}, Serafeim Loukas^{a,c}, Lara Lordier^a, Laura Gui^d, François Lazeyras^d, Petra S. Hüppi^{a,*}

^a Division of Development and Growth, Department of Woman, Child and Adolescent, University Hospitals of Geneva, Geneva, Switzerland

^b Institute of Mathematics, Ecole Polytechnique Fédérale de Lausanne, Lausanne, Switzerland

^c Institute of Bioengineering, Ecole Polytechnique Fédérale de Lausanne, Lausanne, Switzerland

^d Department of Radiology and Medical Informatics, Center of BioMedical Imaging (CIBM), University of Geneva, Geneva, Switzerland

ARTICLE INFO

Keywords:

Diffusion magnetic resonance imaging
Connectomics
Graph-theory
Human brain development
Preterm birth

ABSTRACT

Prematurity disrupts brain development during a critical period of brain growth and organization and is known to be associated with an increased risk of neurodevelopmental impairments. Investigating whole-brain structural connectivity alterations accompanying preterm birth may provide a better comprehension of the neurobiological mechanisms related to the later neurocognitive deficits observed in this population.

Using a connectome approach, we aimed to study the impact of prematurity on neonatal whole-brain structural network organization at term-equivalent age. In this cohort study, twenty-four very preterm infants at term-equivalent age (VPT-TEA) and fourteen full-term (FT) newborns underwent a brain MRI exam at term age, comprising T2-weighted imaging and diffusion MRI, used to reconstruct brain connectomes by applying probabilistic constrained spherical deconvolution whole-brain tractography. The topological properties of brain networks were quantified through a graph-theoretical approach. Furthermore, edge-wise connectivity strength was compared between groups.

Overall, VPT-TEA infants' brain networks evidenced increased segregation and decreased integration capacity, revealed by an increased clustering coefficient, increased modularity, increased characteristic path length, decreased global efficiency and diminished rich-club coefficient. Furthermore, in comparison to FT, VPT-TEA infants had decreased connectivity strength in various cortico-cortical, cortico-subcortical and intra-subcortical networks, the majority of them being intra-hemispheric fronto-paralimbic and fronto-limbic. Inter-hemispheric connectivity was also decreased in VPT-TEA infants, namely through connections linking to the left precuneus or left dorsal cingulate gyrus – two regions that were found to be hubs in FT but not in VPT-TEA infants. Moreover, posterior regions from Default-Mode-Network (DMN), namely precuneus and posterior cingulate gyrus, had decreased structural connectivity in VPT-TEA group.

Our finding that VPT-TEA infants' brain networks displayed increased modularity, weakened rich-club connectivity and diminished global efficiency compared to FT infants suggests a delayed transition from a local architecture, focused on short-range connections, to a more distributed architecture with efficient long-range connections in those infants. The disruption of connectivity in fronto-paralimbic/limbic and posterior DMN regions might underlie the behavioral and social cognition difficulties previously reported in the preterm population.

1. Introduction

Dynamic macrostructural and microstructural changes take place from the mid-fetal stage to birth. Indeed, the third trimester of gesta-

tion is characterized by a rapid brain growth, with gray-matter (GM) and white matter (WM) volume expansion driven by increasing density, diameter and myelination of both dendritic and axonal structures (Dubois et al., 2008; Innocenti and Price, 2005; Kiss et al., 2014;

Abbreviations: CSD, constrained spherical deconvolution; DCG, dorsal cingulate gyrus; DGM, deep gray-matter; dMRI, diffusion magnetic resonance imaging; FA, fractional anisotropy; fMRI, functional magnetic resonance imaging; FT, full-term; GM, gray-matter; OFC, orbito-frontal cortex; PCG, posterior cingulate gyrus; PCUN, precuneus; RC, rich-club; SC, streamline counting; SW, small-world index, TEA, term-equivalent age; TPO, temporal pole; VPT-TEA, very preterm infants at term-equivalent age; WM, white matter.

* Corresponding author.

E-mail address: petra.huppi@hcuge.ch (P.S. Hüppi).

<https://doi.org/10.1016/j.neuroimage.2020.117440>

Received 4 May 2020; Received in revised form 8 September 2020; Accepted 5 October 2020

Available online 8 October 2020

1053-8119/© 2020 The Authors. Published by Elsevier Inc. This is an open access article under the CC BY-NC-ND license (<http://creativecommons.org/licenses/by-nc-nd/4.0/>)

Mills et al., 2016; Nossin-Manor et al., 2013), as well as the establishment of functional thalamocortical and other long-range brain connections (Batalle et al., 2017; Kostovic and Jovanov-Milosevic, 2006; Kostovic and Judas, 2010; Kostovic et al., 2014; van den Heuvel et al., 2015).

Preterm birth disrupts brain maturation during a critical period of fetal brain growth (Kiss et al., 2014; Radley and Morrison, 2005). It impacts typical brain developmental processes, as a result of complex environmental factors (Simmons et al., 2010), leading consequently to structural brain alterations. These alterations might be at the origin of the later neurodevelopmental impairments observed in preterm infants, comprising motor, cognitive, behavioral and socio-emotional deficits (Anjari et al., 2007; Ball et al., 2012; Cismaru et al., 2016; Huppi et al., 1998; Inder et al., 2005; Montagna and Nosarti, 2016; Thompson et al., 2007, 2013).

Magnetic resonance imaging (MRI) has been employed to study the early brain developmental anomalies observed in preterm infants. Such anomalies have been shown to be associated with specific neuropsychological deficits after preterm birth and include regional cortical and subcortical volumetric changes (Ball et al., 2017; Cismaru et al., 2016; Huppi and Dubois, 2006; Ment et al., 2009; Nosarti, 2013; Padilla et al., 2015; Peterson et al., 2000), as well as alterations of brain WM networks and their microstructural characteristics (Ball et al., 2014; Batalle et al., 2017; Fisch-Gomez et al., 2015; Mullen et al., 2011; Pannek et al., 2018; Pecheva et al., 2018; Rogers et al., 2012; Sa de Almeida et al., 2019).

Previous studies have focused mostly on regional brain structural differences between very preterm infants at term-equivalent age (VPT-TEA) and full-term born infants (FT). To date, there is still limited knowledge regarding whole-brain structural alterations at term-equivalent age (TEA) following preterm birth.

The macroscopic whole-brain structural network organization can be investigated using a connectomic analysis, where brain networks are derived by whole-brain tractography, through reconstruction of WM connections between brain regions using brain diffusion MRI (dMRI). In the resulting connectome, brain regions are represented by nodes and the structural connections between brain regions by edges. The edge weights can be either the number of streamlines connecting two regions (SC) or can be defined by measures of microstructural organization, such as fractional anisotropy (FA).

Graph-based measures allow us to study brain network topology, revealing meaningful information regarding small-worldness, integration, segregation, modular organization, the presence of hubs and rich-club connectivity (Bullmore and Sporns, 2009; He and Evans, 2010; Meunier et al., 2010; van den Heuvel and Sporns, 2013). These network measures have been shown to be reliable biomarkers for discriminating normal and abnormal brain networks (Lo et al., 2010; Owen et al., 2013; Shu et al., 2011). Moreover, alterations in structural connectivity have been related to a range of developmental disorders (Crossley et al., 2015; van den Heuvel et al., 2013).

To date, only three studies have used a connectomic analysis to reconstruct whole-brain networks of VPT-TEA and FT infants and compare their topological organization at term age using graph-analysis. In particular, Ball et al., using unweighted brain connectomes, have focused mainly on rich-club connectivity and have found that, although it was intact following preterm birth, VPT-TEA had a greater proportion of direct cortico-cortical connections within the rich-club than FT infants, what was interpreted as a measure of altered deep gray-matter (DGM) connectivity. In addition, brain networks of VPT-TEA infants evidenced increased local connectivity between peripheral nodes, correlating with increased network segregation (Ball et al., 2014). Lee et al. and Brown et al., using weighted brain connectomes, have also addressed this question using graph theoretical measures (Brown et al., 2014; Lee et al., 2019). Lee et al. have found a decreased network global efficiency in VPT-TEA infants in comparison to FT newborns (Lee et al., 2019). On the other hand, Brown et al. have found an increased global network efficiency and modularity in VPT-TEA infants. However, they have com-

pared their own cohort of VPT-TEA infants to an external cohort of FT infants from a previously published study (Yap et al., 2011) and have stated that their findings were resulting from differences in image acquisition and connectome construction pipelines (Brown et al., 2014). Therefore, literature is still not completely clear regarding this matter and lacking a more complete graph-based analysis between the brain networks of VPT-TEA and FT infants. Additionally, there are no reports regarding hub differences and there is only one study evaluating whole-brain edge-wise connectivity strength differences between these groups at term age (Pannek et al., 2013). Further information on this topic would thus be of great importance for understanding the impact of preterm birth on global brain network organization and connectivity at TEA.

In this study, we constructed weighted structural connectomes of a cohort of VPT-TEA and FT infants using dMRI whole-brain probabilistic constrained spherical deconvolution (CSD)-based tractography. We aimed to study whole-brain network topological alterations related to prematurity by employing graph-based analysis on weighted structural networks and comparison of brain network hubs and edge-wise connectivity differences between these two groups of infants. Capitalizing on the latest methodological advances, we intended to contribute to the described gap in the literature regarding this subject.

We hypothesize that, in comparison to FT neonates, VPT-TEA infants' structural connectomes will reveal macroscale brain network differences related to the disruption of early brain development by preterm birth.

2. Materials and methods

2.1. Subjects

A cohort of thirty-nine very preterm (VPT) infants (gestational age (GA) at birth <32 weeks) and twenty-four FT infants was recruited at the neonatal unit of the University Hospitals of Geneva (HUG), Switzerland, from 2013 to 2016, in order to evaluate the impact of prematurity on brain development and clinical neurodevelopment. The study was approved by the local Research Ethics Committee and written parental consent was obtained before the infants' participation to the study. All subjects underwent an MRI examination at TEA (37–42 weeks GA). Infants whose MRI protocol acquisition was incomplete, not comprising a T2-weighted image and/or dMRI sequence, or that presented major focal brain lesions were excluded from the analysis.

The final sample used in this case-control study was of 24 VPT and 14 FT infants. As expected, VPT infants' GA at birth, weight, height and head circumference at birth, as well as APGAR scores were significantly inferior to those of FT newborns. Additionally, presence of bronchopulmonary dysplasia was significantly superior in VPT infants. No significant differences between VPT and FT groups were found in the following demographic and perinatal variables: sex, intrauterine growth restriction, intraventricular hemorrhage (grade I-IV), neonatal asphyxia, blood culture positive sepsis, gestational age at MRI and socioeconomic parental status (Largo et al., 1989) (Table 1).

2.2. MRI acquisition

All infants were scanned after receiving breast or formula feeding, during natural sleep (no sedation used) and using a vacuum mattress for immobilization. MR-compatible headphones were used (MR confon, Magdeburg, Germany) to protect infants from the scanner's noise. All infants were monitored for heart rate and oxygen saturation during the entire scanning time.

MRI acquisition was performed on 3.0T Siemens MR scanners (Siemens, Erlangen, Germany): Siemens TIM Trio with a 32-channel head coil and Siemens Prisma with a 64-channel head coil. Chi-squared test revealed no significant difference regarding the distribution of scanner/coils between groups, $\chi^2(1) = 1.057$, $p = 0.304$ (TIMTrio-32channel: FT=11, VPT=15; Prisma-64channel: FT=3, VPT=9).

Table 1.
Clinical characteristics of the infants.

Clinical characteristics	FT <i>n</i> = 14	VPT-TEA <i>n</i> = 24	<i>p</i> -value* FT vs. VPT-TEA
Gestational age at birth, weeks, mean (SD)	39.2 (± 1.3)	28.3 (± 2.5)	0.0001*
Gestational age at birth, weeks, range	37 ^{2/7} – 41 ^{5/7}	23 ^{6/7} – 32 ^{0/7}	
Sex: female (%) / male (%)	6(15.8) / 8(21.1)	10(26.3) / 14(36.8)	0.943
Birth weight, gram, mean (SD)	3223.6 (± 440.5)	1077.5 (± 328.7)	0.0001*
Birth height, centimetre, mean (SD)	49.8 (± 1.7)	36.2 (± 3.6)	0.0001*
Birth head circumference (cm), mean (SD)	34.3 (± 1.1)	25.8 (± 2.6)	0.0001*
APGAR score, 1 min (SD)	8.9 (± 0.5)	4.8 (± 3.1)	0.0001*
APGAR score, 5 min (SD)	9.5 (± 0.9)	7.1 (± 1.9)	0.0001*
Intrauterine Growth Restriction, <i>n</i> (%)	1 (2.6)	3 (7.9)	0.604
Bronchopulmonary dysplasia (%)	0 (0.0)	7 (18.4)	0.025*
Intraventricular Hemorrhage grade I-II (%)	0 (0.0)	5 (13.2)	0.067
Intraventricular Hemorrhage grade III-IV (%)	0 (0.0)	0 (0.0)	
Neonatal asphyxia, <i>n</i> (%)	0 (0.0)	0 (0.0)	
Blood culture positive Sepsis (%)	0 (0.0)	5 (13.2)	0.067
Gestational age at MRI scan, weeks, mean (SD)	39.6 (± 1.2)	40.3 (± 0.6)	0.073
Gestational age at MRI scan, weeks, range	37 ^{2/7} – 42 ^{0/7}	39 ^{1/7} – 41 ^{1/7}	
Socioeconomic score (range 2–12), mean (SD)	4.10 (± 2.5)	5.67 (± 3.1)	0.169

* Group-characteristics were compared using independent samples T-test for continuous variables and chi-squared test for categorical variables.

Table 2.
Group-wise comparison of dMRI motion metrics.

Motion metrics	FT <i>n</i> = 14	VPT-TEA <i>n</i> = 24	<i>p</i> -value* FT vs. VPT-TEA
Number of outliers, mean percentage (SD)	3.24 (± 1.68)	3.05 (± 2.33)	0.789
Number of outliers, percentage, range	0.87 – 6.22	0.22 – 9.67	
Absolute between volumes motion, mm (SD)	1.40 (0.46)	1.39 (0.49)	0.950
Absolute between volumes motion, mm, range	0.60 – 2.30	0.64 – 2.41	
Relative between volumes motion, mm (SD)	0.66 (± 0.30)	0.76 (± 0.38)	0.375
Relative between volumes motion, mm, range	0.16 – 1.21	0.25 – 1.88	

* Motion metrics were compared between groups using independent samples T-test.

T2-weighted images were acquired using the following parameters: 113 coronal slices, TR=4990 ms, TE=151 ms, flip angle=150°, matrix size=256 × 164; voxel size=0.4 × 0.4 × 1.2 mm³, total scan time of 6:01 minutes. dMRI was acquired with a single-shot spin echo-planar imaging (SE-EPI) Stejskal-Tanner sequence (TE=84 ms, TR= 7400 ms, acquisition matrix 128 × 128 mm, reconstruction matrix 128 × 128 mm, 60 slices, voxel size 2 × 2 × 2 mm³). Images were acquired in the axial plane, in anterior-posterior (AP) phase encoding (PE) direction, with diffusion gradients applied in 30 non-collinear directions with a b-value of 1000 s/mm² and one non-diffusion weighted image (*b* = 0), with a total scan time of 4:12 minutes. dMRI motion metrics estimates per subject, including percentage of outliers, as well as relative and absolute between volumes motion, were calculated using EDDY QC tools from diffusion toolbox of the FMRIB Software Library, FSL v6.0.3, <https://fsl.fmrib.ox.ac.uk/fsl/fslwiki/> (Behrens et al., 2003; Smith et al., 2004). No statistically significant differences between groups were found for any of the motion metrics (Table 2, Supplementary Fig. S1).

2.3. Pre-processing

T2-weighted brain volumes were bias-corrected, skull-stripped and tissue-segmented into WM, GM, DGM, cerebrospinal fluid (CSF) and cerebellum using an automatic neonatal-specific segmentation algorithm (Gui et al., 2012). dMRI data were preprocessed using the diffusion toolbox of the FMRIB Software Library, FSL v5.0.10, <https://fsl.fmrib.ox.ac.uk/fsl/fslwiki/> (Behrens et al., 2003; Smith et al., 2004). Brain extraction was performed using “BET”. Eddy current-induced distortions and gross subject movement were corrected using the FSL “EDDY” tool (Andersson and Sotiropoulos, 2016) optimized for neonatal dMRI data. This command is part of the neonatal dMRI automated pipeline from the developing Human Connectome Project and corrects distortions caused by motion-induced signal dropout and intra-

volume subject movement (Andersson et al., 2016, 2017; Bastiani et al., 2019).

2.4. Network nodes definition: brain parcellation

Parcellation into cortical and subcortical regions was based on the UNC neonatal brain atlas (Shi et al., 2011), consisting of 90 regions, which represented the nodes used in the network analysis.

The T2 UNC neonatal brain atlas (Shi et al., 2011) was registered to each subject’s T2-weighted structural image by means of a non-linear registration using the advanced normalization tools (ANTs) package (Avants et al., 2011) adapted for neonatal data (Bastiani et al., 2019). Subject’s dMRI data was registered to the T2-weighted structural image by means of FSL FLIRT (Jenkinson et al., 2002). All the registrations were individually visually inspected in order to guarantee the quality of the process.

We then combined the linear transformation (subject’s dMRI to T2 structural) with the non-linear warp registration (subject’s T2 structural to T2 atlas) to obtain the transformations needed to bring the T2 atlas to subjects’ dMRI space. Therefore, the anatomical regions (labels) from the UNC atlas were propagated to each subject’s dMRI space by applying this combined transformation using nearest neighbor interpolation, and used as nodes for network analysis.

2.5. Network edges definition: tractography

In order to reconstruct WM fibers to define network edges, whole-brain tractography was performed in native diffusion space using probabilistic single-shell, single tissue constrained spherical deconvolution (SSST-CSD) tracking. It was performed by means of MRtrix3 (Tournier et al., 2019), using iFOD2, anatomically constrained tractography (ACT) and backtrack re-tracking algorithms, with streamlines seeded dynamically throughout the WM, producing 100 million stream-

lines per subject. Examples of the the overlap between the mrtrix 5TT tissue segmentation image and the subject's native diffusion space (diffusion b0 image) in representative subjects from both preterm and full-term infants' groups can be found in Supplementary Fig. S2. The reconstructed data was then further processed using spherical-deconvolution informed filtering of tractograms (SIFT) algorithm, producing 10 million streamlines for each subject, which were used as brain network edges.

2.6. Network construction and global network analysis

In order to construct the individual WM structural brain networks, the reconstructed set of streamlines were combined with each subject's anatomical parcellation. This resulted in a 90×90 interregional connectivity matrix, where each anatomical region is considered as a node (Supplementary Table S1), and each pair of nodes is connected by an edge, representing the strength of connectivity between the corresponding regions. Self-connections were excluded. For each pair of nodes/regions, we computed the number of filtered streamlines (SC) connecting both regions, as well as the mean fractional anisotropy (FA) along streamlines connecting the regions. In order to remove spurious connections in the SC-weighted (SCw) connectomes, all connections where FA was inferior or equal to 0.1 were considered as noise floor and therefore removed, according to Jones and Basser (2004). This threshold was chosen due to the low anisotropy of the preterm infant's brain and has been applied in previous studies performing structural network analysis in the preterm and neonatal brain (Brown et al., 2014; van den Heuvel et al., 2015; Zhao et al., 2019).

For analysing results from graph network measures, first, for each subject, network weights were normalized by the maximum weight value of that network, in order to normalize all edge weights per subject. The edge weights in SCw networks will represent therefore relative connectivity.

Graph theoretical analysis of SCw connective matrices was performed by using the Brain Connectivity Toolbox (BCT) for Matlab (Rubinov and Sporns, 2010). The metrics evaluated included:

- 1 Density (d): computes the observed connections as a percentage of all possible connections.
- 2 Total strength (S): computed as the sum of the strength (sum of weights) across all the nodes in the network.
- 3 Characteristic path length (L): computed as the average of shortest path lengths between all pairs of nodes in the network (Watts and Strogatz, 1998).
- 4 Global efficiency (GEff): computed as the average inverse of the shortest path lengths (Rubinov and Sporns, 2010).
- 5 Average clustering coefficient (C): clustering coefficient was first computed as the fraction of a node's neighbors that are also connected to each other. These fractions at each node were averaged over all the nodes of the network to give the overall network C (Watts and Strogatz, 1998).
- 6 Local efficiency (LEff): computed as the average of the global efficiency of each node's neighborhood sub-graph, averaged over all the nodes of the network (Latora and Marchiori, 2001).
- 7 Small-world index (SW): computed as the ratio of the normalized C and the normalized L (which were obtained as the ratio between the metrics derived from each subject network and its matched randomized network metrics).
- 8 Modularity index (Q): Louvain algorithm for community detection was used to identify modules in the network (Lu et al. 2015) (Lu. Q was calculated by computing the ratio between the number of connections (sum of edge weights) within the modules and the number of connections exiting the same modules, and taking the maximum of these ratios across all possible modules (Newman, 2004).
- 9 Rich-club (RC) coefficient ($\phi(\kappa)$): computed as proposed by Opsahl et al. for weighted networks (Opsahl et al., 2008). Given a nodal strength κ , we identified the subset of nodes $E_{>\kappa}$ with a nodal

strength $> \kappa$. The weighted $\phi(\kappa)$ was computed as the ratio between the sum of weights of the connections between the nodes present in $E_{>\kappa}$, and the maximal possible weighted connectedness within $E_{>\kappa}$. The chosen κ corresponded to the 9th highest nodal strength per subject, in order to include the top 10% nodes.

In order to remove bias related to the fraction of measure's value that may arrive by chance, we generated 10 matched random equivalent networks for each subject (where each edge was rewired 1000 times), preserving the same number of nodes and degree distributions as in the SCw networks. The network measures of each of the 10 random networks were then averaged per subject and used for normalization.

Normalized (calibrated) C (nC), LEff (nLEff), L (nL), GEff (nGEff) and Q (nQ) were estimated as the ratio between the metrics derived from each subject network and its matched randomized network metrics. The normalized $\phi(\kappa)$ (ϕ_{norm}) was obtained by multiplying $\phi(\kappa)$ by the ratio between the number of nodes included into the RC pool $E_{>\kappa}$ (varying as a function of RC strength κ) and the total number of network nodes. This computation is motivated by the fact that $\phi(\kappa)$ is inversely proportional to the number of nodes included in the RC pool (Karolis et al., 2016).

Group-average weighted structural connectomes and matched randomized network structural connectomes were computed for both VPT-TEA and FT infants' groups. $\phi(\kappa)$ was computed as a function of κ per group for both networks. $\phi(\kappa)_{\text{norm}}$ was computed as the ratio between the $\phi(\kappa)$, for the different levels of κ , of the group-average weighted structural connectome and the $\phi(\kappa)$, for the same levels of κ , of the matched randomized network structural connectomes.

For the detection of hubs within each group's brain networks, group-average binary structural connectomes were computed for both VPT-TEA and FT infants' groups, by including the structural connections that were present in at least 70% of the total group. We used the nodal degree (the number of connections of a node) as a measure to define the hubs. Using BCT, nodal degree was calculated for all nodes of each binary group network. Hubs were identified for each group as the nodes with a nodal degree superior to the average nodal degree plus 1 standard deviation.

2.7. Edge-wise connectivity strength analysis

To evaluate edge-wise connectivity strength differences between groups based on SCw structural networks, we performed t-tests at the connection level with false discovery rate (FDR) control (significance value of 0.05 and 100,000 random permutations). To this end, we used the NBS toolbox implemented in Matlab by Zalesky et al. (Benjamini and Hochberg, 1995; Zalesky et al., 2010).

Connectomic data was visualized using the Circos software (Krzywinski et al., 2009).

Statistically significantly different connections between groups were categorized into: (1) cortico-cortical; (2) cortico-subcortical and (3) subcortico-subcortical.

2.8. Statistical analysis

Neonatal and demographic data, categorical variables (sex, intrauterine growth restriction, bronchopulmonary dysplasia, intraventricular hemorrhage (grade I-IV), blood culture positive sepsis and neonatal asphyxia) were analysed using chi-squared test, whereas continuous variables were compared using independent samples t-test, with group as independent variable and the following dependent variables: GA at birth, GA at MRI, birth weight, birth height, birth head circumference, APGAR score at 1 and 5 min after birth and socioeconomic parental status. dMRI motion metrics were compared between groups using independent samples t-test, with group as independent variable and the following dependent variables: percentage of number of outliers, absolute between volumes motion, relative between volumes motion.

Group-wise differences in network graph-theoretical metrics and number of thalamic connections were investigated with one-way

Table 3.
Global network measures comparison between groups.

Global network measures	VPT-TEA	FT	<i>p</i> -value
d	0.435 (± 0.031)	0.452 (± 0.026)	0.135
S	1.158 (± 0.231)	1.170 (± 0.251)	0.892
nL	2.657 (± 0.675)	2.175 (± 0.391)	0.049
nGEff	0.701 (± 0.068)	0.775 (± 0.039)	0.045
nC	2.827 (± 0.155)	2.618 (± 0.135)	0.001
nLEff	1.522 (± 0.076)	1.416 (± 0.042)	0.0001
SW	1.117 (± 0.232)	1.157 (± 0.115)	0.677
nQ	1.017 (± 0.023)	0.998 (± 0.018)	0.006

One-way ANCOVA, controlling for GA at MRI and sex, was performed to determine differences between groups. Numbers in bold indicate significant results between groups ($p < 0.05$).

between-subjects ANCOVA, controlling for GA at MRI and sex, using IBM SPSS Statistics version 25 (IBM Corp., Armonk, N.Y., USA). One-way between-subjects MANCOVA, controlling for GA at MRI and sex, was performed first, comprising all graph-theoretical metrics analysed, namely network strength, network density, nC, nLEff, nL, nGEff, nQ and ϕ_{norm} , to correct for the multiplicity of global tests.

Independent-samples *t*-test was used to compare Q from SCw networks to Q from its matched random networks.

P-values that resulted from edge-wise comparison of connectivity matrices statistics were corrected using Benjamini-Hochberg FDR control procedure at level alpha of 5%, implemented in the NBS toolbox (Benjamini and Hochberg, 1995; Zalesky et al., 2010).

2.9. Data and code availability

All data were acquired in the context of the research project approved by the ethical committee in 2011. The patient consent form did not include any clause for reuse or share of data. It stated explicitly that all data (clinic, biologic and imaging) would not be used with any other aim apart from the present research study and would not be shared with third parties.

Software and code used in this study are publicly available as part of FSL v5.0.10 (<https://fsl.fmrib.ox.ac.uk/fsl/fslwiki/>), MRtrix3 (Tournier et al., 2019), ANTs (Avants et al., 2011), BCT (Rubinov and Sporns, 2010) and NBS (Benjamini and Hochberg, 1995; Zalesky et al., 2010) software packages. dMRI data were pre-processed using EDDY command adapted for neonatal motion, which is part from the neonatal dMRI automated pipeline from developing Human Connectome Project (dHCP, <http://www.developingconnectome.org>), and can be found at this link: https://git.fmrib.ox.ac.uk/matteob/dHCP_neo_dMRI_pipeline_release (Bastiani et al. 2019).

3. Results

3.1. Preterm neonatal structural brain network topological organization

3.1.1. Integration, segregation and small-world properties

Structural network topology was compared at TEA between VPT-TEA infants and FT newborns using metrics derived from graph-analysis. One-way MANCOVA multivariate test yielded a significant difference between the group contrasts, [Wilks' $\lambda = 0.362$, $F(8,26)=4.182$, $p = 0.005$], when considering all graph metrics. Given the significance of the overall test, the univariate main effects of each metric were examined.

No significant differences were found in mean network density ($p = 0.135$) or total network strength ($p = 0.892$) between FT newborns and VPT-TEA infants' SCw networks (Table 3).

We explored the differences in brain networks integration capacity between FT and VPT-TEA infants using characteristic path length and global efficiency. In comparison to FT newborns, VPT-TEA infants showed a significantly higher normalized characteristic path length

($p = 0.049$) and significantly diminished normalized global efficiency ($p = 0.045$) (Fig. 1A, B, Table 3). Although a similar tendency was observed in networks before normalization with matched random networks, the differences were not statistically significant, $p > 0.05$ (Supplementary Table S2).

Network segregation was measured by means of average cluster coefficient, local efficiency and modularity. In comparison to FT newborns, VPT-TEA infants showed a significantly higher normalized average clustering coefficient, ($p = 0.001$) and significantly higher normalized local efficiency (Fig. 1C, D, Table 3). A similar tendency was observed in networks before normalization with matched random networks, but the differences were not statistically significant, $p > 0.05$ (Supplementary Table S2).

Both FT and VPT-TEA infants presented a modular architecture in their brain networks. This is reflected by $Q > 0.3$ in both groups (Supplementary Table S2), which is indicative of a non-random modular structure (Newman and Girvan, 2004). VPT-TEA infants had a significantly higher nQ ($p = 0.032$) and Q ($p = 0.007$) compared to FT infants (Fig. 1D, Table 3, Supplementary Table S2).

The balance between segregation and integration was quantified by the small-world network topology. Both FT and VPT-TEA infants brain networks had a $SW > 1$, without statistically significant differences between groups (Table 3), proving the small-world organization of the neonatal brain in both groups.

3.1.2. Hubs and rich-club organization

Both FT and VPT-TEA infants' structural brain networks revealed a right-tailed distribution of nodal degree, suggestive of the existence of densely connected nodes, hubs (Fig. 2A and B).

We found 9 hubs in FT infants with an average nodal degree of 51.67, whereas VPT-TEA infants presented a higher number of hubs, namely 16, but with an inferior average number of connections (average nodal degree of 45.38). The hub regions in both groups consisted of mainly subcortical (thalamus, caudate and putamen) and limbic (dorsal cingulate gyrus, insula and hippocampus) nodes. Noticeably, FT newborns had a parietal hub (left precuneus) not present in VPT-TEA infants, whereas VPT-TEA infants had temporal hubs not present in FT newborns (bilateral superior temporal gyrus and left Heschl gyrus), as well as both amygdalae as hubs (Fig. 3, Supplementary Table S3). The following hubs were discovered in VPT-TEA infants: bilateral thalamus, bilateral caudate, bilateral putamen, bilateral hippocampus, bilateral insula, bilateral amygdala, right dorsal cingulate gyrus, left Heschl gyrus and bilateral superior temporal gyrus. The following hubs were present in FT newborns: bilateral thalamus, left caudate, right putamen, right insula, right hippocampus, bilateral dorsal cingulate gyrus and left precuneus (Supplementary Table S3).

For both groups, left and right thalamus were the two regions with highest nodal degree (Supplementary Table S3). When comparing the number of connections of these two regions, combined, between VPT-TEA and FT infants, the VPT-TEA showed a statistically significantly lower number of connections of the left and right thalamus in comparison to FT infants ($p = 0.025$) (Fig. 2C).

Normalized rich-club curves, representative of both FT and VPT-TEA groups, show an increasing ϕ_{norm} with the increase of κ for both groups. This increase is superior for FT infants, in comparison to VPT-TEA infants, at the strongest network nodes (from $\kappa=45$ to $\kappa=60$) (Fig. 2E). Both the FT and VPT-TEA infants' brain networks displayed RC organization, with $\phi_{\text{norm}}(\kappa) > 1$ for $\kappa \geq 9$. Considering the top 10% strongest network nodes, FT infants presented both a statistically significantly higher ϕ_{norm} ($p = 0.007$) and ϕ ($p = 0.003$) in comparison to VPT-TEA infants (Fig. 2D, Supplementary Table S2).

3.2. Prematurity and the connectivity strength of structural networks

In comparison to FT, the VPT-TEA infants brain networks presented 90 connections (out of the total 4005 unique possible connections)

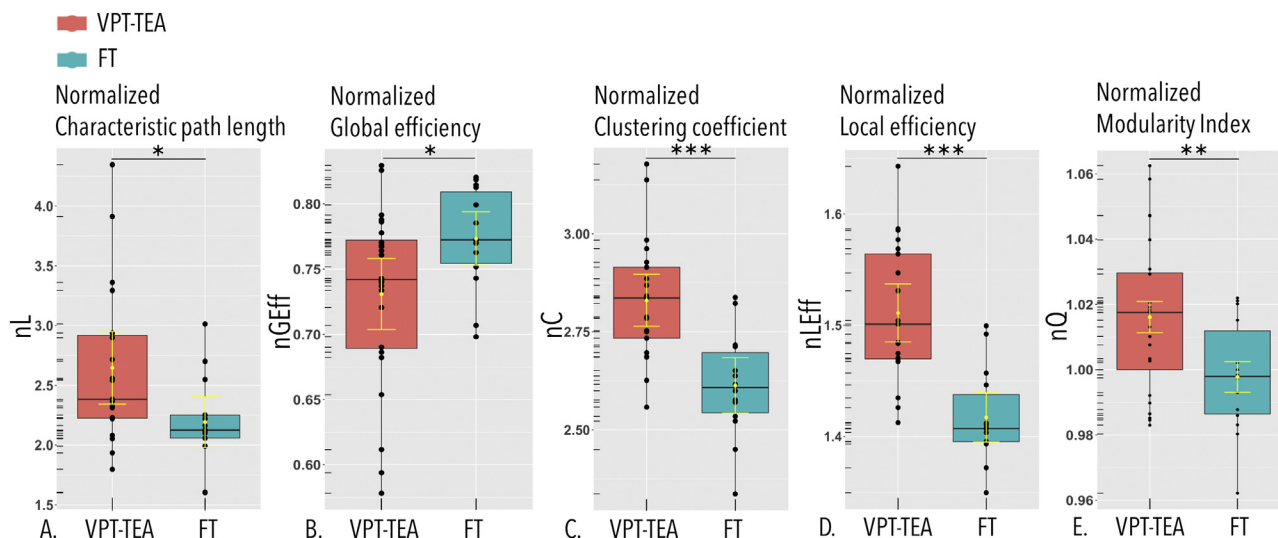


Fig. 1. Global network measures differences between VPT-TEA and FT infants. Boxplots of global network measures in VPT-TEA (in red) and FT infants (in green): normalized characteristic path length, nL (A), normalized global efficiency, nGEff (B), normalized cluster coefficient, nC (C), normalized local efficiency, nLEff (D), and normalized modularity index, nQ (E). One-way ANCOVA, controlling for GA at MRI and sex, was performed to determine differences between groups. Mean and standard deviation are illustrated in yellow on each boxplot. Lines indicate significant differences between groups (* $p < 0.05$, ** $p < 0.01$, *** $p < 0.001$).

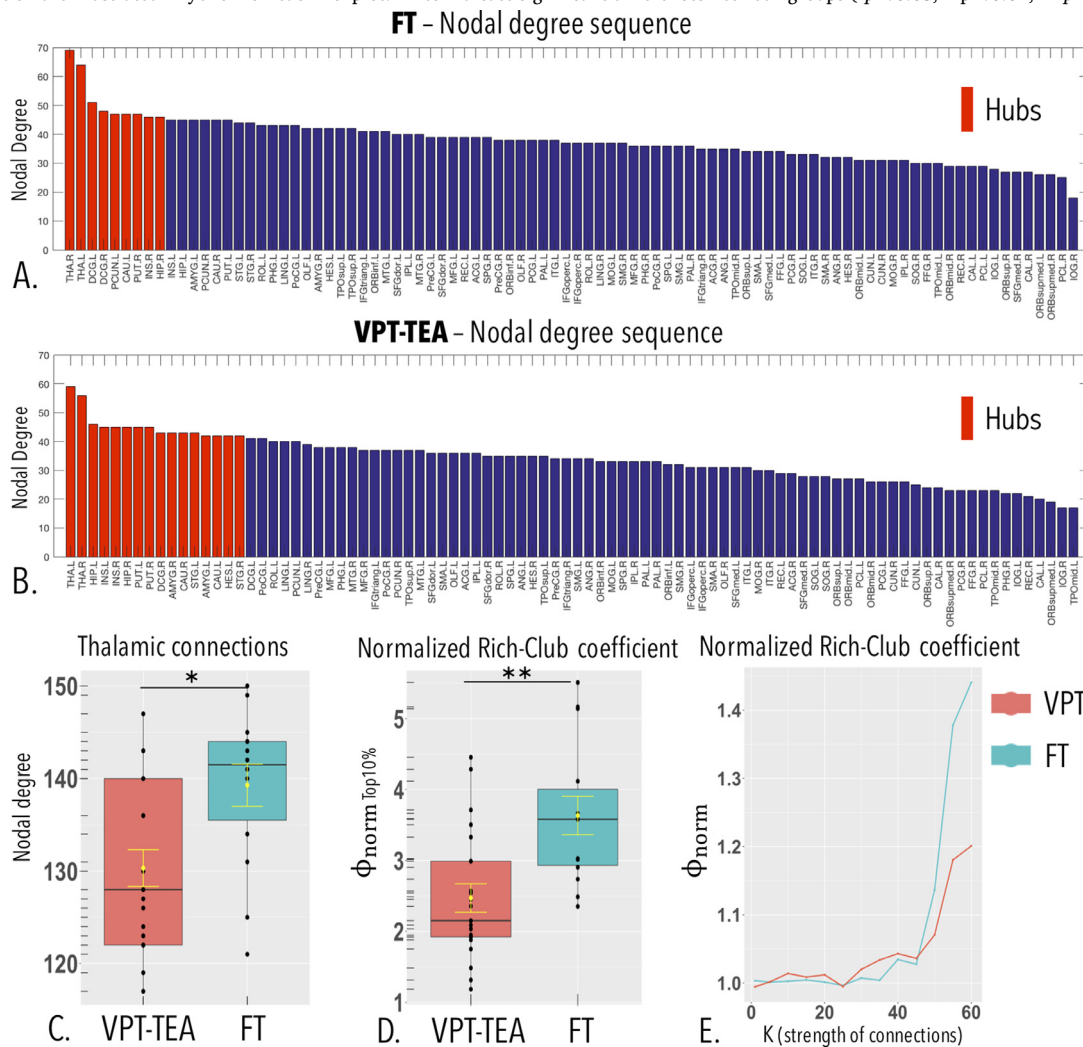


Fig. 2. Hubs, thalamic connectivity and rich-club organization. A and B: Structural brain hubs of FT (A) and VPT-TEA (B) infants. Hubs (in red) were defined as nodes whose degree was ≥ 1 standard deviation above the average nodal degree. C and D: Boxplots of mean thalamic connections (C) and normalized rich-club coefficient of the top 10% strongest network nodes ($\phi_{norm}^{Top10\%}$) (D) in VPT-TEA and FT infants. One-way ANCOVA, controlling for GA at MRI and sex, was performed to determine differences between groups. Mean and standard deviation are illustrated in yellow on each boxplot. Lines indicate statistically significant differences between groups (* $p < 0.05$, ** $p < 0.01$). E: Normalized rich-club curves (ϕ_{norm}) of FT and VPT-TEA infant's representative weighted networks.

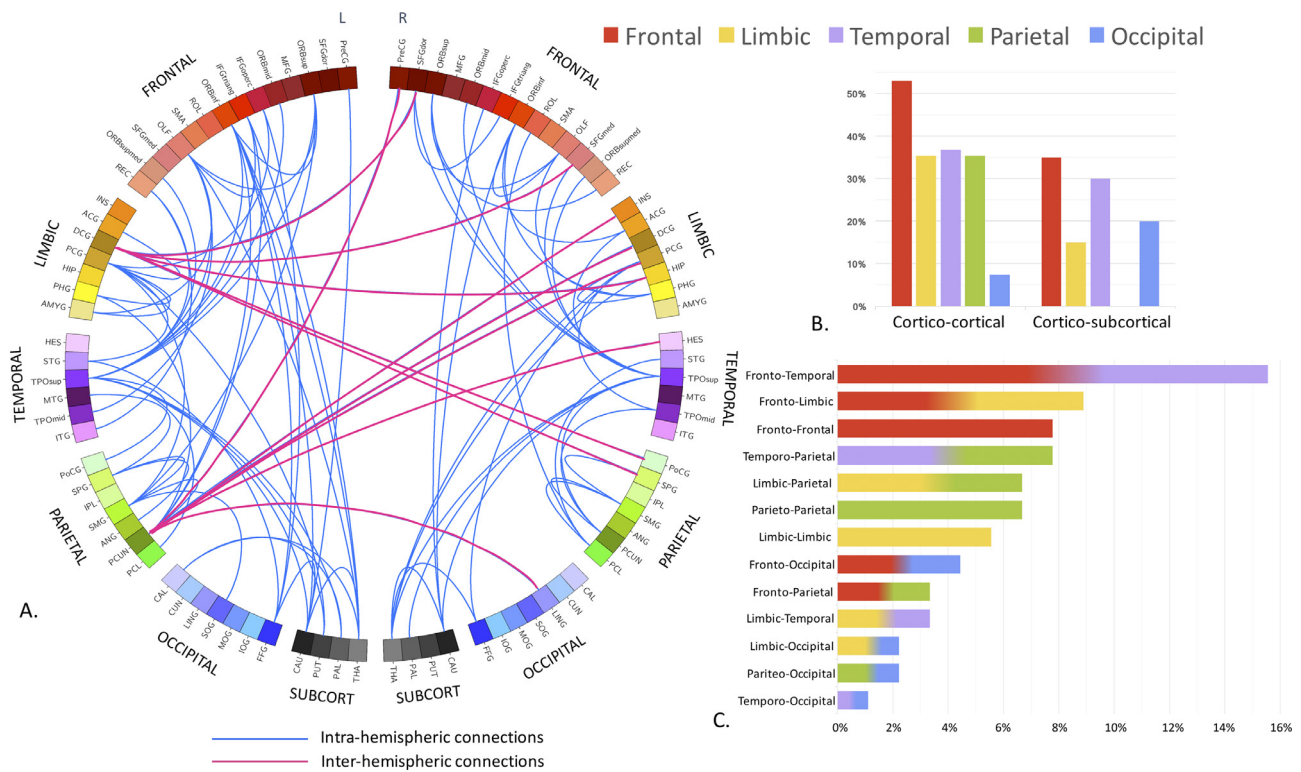


Fig. 3. Brain network connections with significant diminished structural connectivity in prematurely born neonates. A. Representation of brain network connections with a statistically significantly decreased structural connectivity strength in VPT-TEA in comparison to FT infants. Intra-hemispheric connections are represented in blue while inter-hemispheric in pink. Visualization made using the Circos software (Krzywinski et al., 2009). B. Bar graph representation of the relative percentual distribution of cortical nodes participating in the cortico-cortical and cortico-subcortical connections with a diminished connectivity strength in VPT-TEA in comparison to FT infants. C. Bar graph representing the relative percentual distribution of cortico-cortical connections with a diminished connectivity strength in VPT-TEA in comparison to FT infants.

with a statistically significant decreased structural connectivity strength ($p < 0.05$, FDR corrected). These included both intra-hemispheric (88%, out of which 51% in the left and 37% in right hemisphere) and inter-hemispheric (12%) connections (Fig. 3A). A complete description of all connections with decreased structural connectivity strength in VPT-TEA can be found in Supplementary Table S4.

In both cortico-cortical and cortico-subcortical connections, the cortical nodes participating in the connections with decreased connectivity strength in VPT-TEA infants belonged mostly to the frontal cortex. In cortico-cortical connections, these were followed by temporal, limbic, parietal and occipital cortices, and in cortico-subcortical connections, by the temporal, occipital and limbic cortices (Fig. 3B).

Among the fronto-cortical and fronto-subcortical connections with decreased connectivity strength in VPT-TEA infants, the orbito-frontal cortex (OFC) was the frontal node the most frequently involved (participating in 44% of all fronto-cortical/subcortical connections) (Supplementary Table S5 and S6).

Fronto-temporal connections were the most frequently affected, not only among fronto-cortical, but among all cortico-cortical connections (Fig. 3C, Supplementary Table S5). Out of those, 93% were connecting to the temporal pole (TPO). Indeed, connections from the OFC to the TPO were the most frequent (50%) among all frontal-temporal connections with decreased connectivity strength in VPT-TEA, as well as among all fronto-cortical connections (almost 20% of these) (Supplementary Tables S4 and S5). Noticeably, the TPO was the region most frequently involved in all connections with decreased connectivity strength in VPT-TEA infants, followed by the OFC (Supplementary Tables S7).

The fronto-limbic connections were the second most affected cortico-cortical connections after fronto-temporal connections. The cingulate gyrus was the limbic region most frequently present, not only in the af-

fected fronto-limbic connections, but among all limbic connections with decreased connectivity strength in VPT-TEA infants, in particular the posterior cingulate gyrus (PCG) (Fig. 3C, Supplementary Tables S4–S7). Indeed, the PCG was the third most frequent region among all connections with decreased connectivity strength in VPT-TEA infants, after the TPO and OFC (Supplementary Table S7).

Of notice, the precuneus (PCUN), the fourth most frequent region among all connections with decreased connectivity strength in VPT-TEA infants, was the most frequent region participating in all parieto-cortical affected connections (Supplementary Tables S6 and S7). Furthermore, the left PCUN was the node the most frequently involved in inter-hemispheric connections with decreased connectivity strength in VPT-TEA infants, followed by the left dorsal cingulate gyrus (DCG) (Supplementary Table S4).

4. Discussion

In this study, using a connectome approach, we explored whole-brain network topological alterations using graph-based analysis and edge-wise connectivity strength in order to compare brain structural connectivity alterations on VPT-TEA infants and FT newborns and thus assess the impact of prematurity on whole-brain structural organization at TEA.

The major findings from this study are: 1) VPT-TEA infants' brain networks presented an increased characteristic path length, decreased global efficiency, increased clustering coefficient and increased modularity index, reflecting increased segregation and decreased integration in comparison to FT newborns; 2) Altered connectivity of typical neonatal network hubs, in particular the thalamus, left PCUN and left DCG, as well as a diminished rich-club coefficient in VPT-TEA infants' brain net-

works; 3) Decreased connectivity of fronto-paralimbic and fronto-limbic connections, in particular of the orbitofrontal-temporal pole circuitry, as well as of DMN posterior regions, such as the PCUN and PCG, in VPT-TEA infants' brain networks in comparison to FT infants.

4.1. Prematurity is associated with an immature brain structural network topological organization at TEA

4.1.1. Increased segregation and decreased integration of brain networks in prematurely born neonates

The topological organization of the brain structural network has been investigated in fetal and preterm infants throughout development. From the second trimester to TEA, various studies have shown an increase in network strength and integration capacity, with a decrease of characteristic path length and increase of network global efficiency, both during normal fetal (Song et al., 2017) as well as preterm brain development (Ball et al., 2014; Bataille et al., 2017; Brown et al., 2014; van den Heuvel et al., 2015; Zhao et al., 2019). Characteristic path length and network global efficiency refer to the ability of communication between distributed nodes and thus reflect the global information transfer efficiency (Rubinov and Sporns, 2010). Indeed, during fetal brain development, there is a dramatic growth of major long association WM fibers from 20 to 40 weeks GA, which is thought to underlie the dramatic increases of network strength and efficiency (Song et al., 2017). Since preterm birth occurs during this critical period of brain development, it might impact normal topological network organization, namely by disrupting the establishment of long-range structural connections. This could explain the significantly higher characteristic path length and significantly diminished global efficiency that we found at term age in the brain networks of VPT-TEA infants in comparison to FT newborns, what is in line with previous literature findings (Ball et al., 2014; Fisch-Gomez et al., 2015; Lee et al., 2019; Thompson et al., 2016).

Literature has suggested that the typical developmental course of the brain structural network is characterized by a progressive maturational shift from short-range to long-distance connections, with a continuously increasing integration and decreasing segregation with age, favoring thus an integrative topology (Hagmann et al., 2010; Huang et al., 2015; Tymofiyeva et al., 2013; Yap et al., 2011). Network segregation relates to its organization into a collection of sub-networks and can be measured by means of average clustering coefficient, local efficiency and modularity. During early development, a decreasing clustering coefficient has been observed both in fetal development, from 20 to 35 weeks GA (Song et al., 2017), as well as in preterm development between 30 and 40 weeks GA (Ball et al., 2014). In this study, we found that VPT-TEA infants showed a significantly higher clustering coefficient and local efficiency in comparison to FT newborns, which confirms previous reported findings (Ball et al., 2014) and suggests that the expected decrease in brain network segregation described during normal development is affected by preterm birth. In non-normalised networks, a tendency for an increased characteristic path length, diminished global efficiency and increased clustering coefficient and local efficiency was also observed in FT newborns, in comparison to VPT-TEA infants, although not statistically significant, what can be related to the reduced study sample size.

Additionally, modularity index revealed that both VPT-TEA and FT groups had a modular network organization, in which nodes are highly connected to one another within the same community and sparsely connected to nodes in other communities (Newman, 2004). However, we found an increased modularity index in VPT-TEA infants compared to FT newborns. Modularity has been shown to decrease along development, with an increase of communications between different modules from birth to adolescence (Huang et al., 2015). Our results indicate for the first time that prematurity leads to an increase of structural brain network modularity at TEA, with network nodes holding more connections within nodes from the same module than with nodes from other

modules, what supports the increased segregation and decreased integration observed in VPT-TEA infants' brain networks.

An optimal balance between segregation and integration is ideal to allow high capacity for local and global information transfer. This aspect was quantified by the small-world network topology. No differences were found between VPT-TEA and FT infants regarding the SW index, which was >1 in both cases, suggesting a generally efficient local and global organization in both groups.

Summing up, our data reveals that the brain of a VPT infant at TEA, in comparison to a FT newborn, evidences a topological organization corresponding to a typical earlier stage of development, with decreased integration and increased segregation properties. Integration of distributed neuronal activity across specialized brain systems is required for higher brain function and supports diverse cognitive processes, such as language (Friederici and Gierhan, 2013), emotion (Pessoa, 2012), cognitive control (Power and Petersen, 2013) and learning (Bassett et al., 2011, 2015), skills known to be impaired in infants that were born preterm (Anderson and Doyle, 2003; Bhutta et al., 2002; Marlow, 2004; Montagna and Nosarti, 2016; Spittle et al., 2009, 2011; Witt et al., 2014). The fact that VPT-TEA infants' structural brain networks were found to be more modular and less globally efficient than in FT newborns might result from different factors potentially associated with preterm birth, such as a disruption of the activity-dependent synaptic pruning, of the growth and maturation of major long-range association WM fibers, or an impaired reinforcement of the maturation of WM connections. Such factors could explain the observed delayed shift from a local emphasis, based on short-range connections, to a more distributed brain network architecture, based on long-range connections.

Topological characteristics of structural brain networks observed early in development, including network integration and segregation measures, such as global efficiency and clustering coefficient, have been found, respectively, to be significantly correlated with cognitive performance (Keunen et al., 2017) and internalizing and externalizing behaviours assessed in early childhood (Wee et al., 2017). These findings support the hypothesis that the altered global brain network organization observed in VPT-TEA infants might underlie the neurodevelopmental impairments reported in preterm-born infants at later ages.

4.1.2. Brain network hubs differences and impaired rich-club organization in prematurely born neonates

Connections within the connectome can be distributed unevenly, such that certain nodes possess a larger number of connections than others, which makes them network hubs (van den Heuvel and Sporns, 2013). Brain network hubs play a central role in facilitating the integration of disparate neural systems, namely by forming long-range connections (van den Heuvel and Sporns, 2011; van den Heuvel et al., 2012). Structural hubs have been shown to be present already during the prenatal period and to have a consistent spatial topography throughout development (Ball et al., 2014; Chen et al., 2013; Hagmann et al., 2010).

Our results confirm that by term age, both FT and VPT-TEA infants' brain networks demonstrate the presence of network hubs, comprising mainly subcortical (thalamus, caudate and putamen) and limbic (dorsal cingulate gyrus, insula and hippocampus) regions in both groups. Interestingly, the left PCUN was detected as a hub only in FT infants, whereas the bilateral superior temporal gyrus, left Heschl gyrus and both amygdalae were identified as hubs only in VPT-TEA infants. Most of these regions have already been reported as network hubs in neonates and many of them have been shown to persist throughout development (Ball et al., 2014; Chen et al., 2013; Huang et al., 2015; Pandit et al., 2014; van den Heuvel and Sporns, 2011; van den Heuvel et al., 2015).

From all detected network hubs, the left and right thalamus were the two regions with the highest nodal degree in both VPT-TEA and FT newborns. Of notice, VPT-TEA infants presented a significantly diminished number of thalamic connections in comparison to FT infants, which is in agreement with previous literature evidencing diminished thalam-

cortical connectivity and reduced network capacity of DGM following preterm birth (Ball et al., 2013, 2014, 2015). Moreover, this diminished connectivity might contribute to the reduced integration capacity observed in VPT-TEA infants' brain networks. Thalamocortical connections are established during the late second and third trimester of development, when preterm birth occurs (Kostovic et al., 2002, 2014), and therefore prematurity and its associated events, such as inflammation, hypoxia/ischemia, stress and important environmental changes, may affect the establishment of these connections. The thalamus, as a subcortical hub, has been shown to present a rich-club connectivity pattern, to be involved in large-scale integration of neural signals (Alexander et al., 1986; van den Heuvel and Sporns, 2011) and in important higher-order cognitive functions (Bressler, 1995; Bressler and Menon, 2010). In particular, an impaired thalamocortical structural connectivity at TEA, following preterm birth, has been shown to correlate with impaired cognitive performance in premature infants at two years of age (Ball et al., 2015). Additionally, at school age, alterations in the cortico-basal ganglia-thalamo-cortical loop (namely prefrontal-subcortical circuits), following preterm birth, were associated with poorer social behavior, recognition of social context and simultaneous information processing at school age (Fischi-Gomez et al., 2015).

The left PCUN, a hub that we observed in FT but not in VPT-TEA infants, has already been shown to be a network hub in the newborn brain (Huang et al., 2015; Yap et al., 2011). The PCUN is a brain region situated in a strategic location with wide-spread connections and is suggested to be a major association area, supporting a variety of behavioural functions (Cavanna and Trimble, 2006), including memory retrieval (Lundstrom et al., 2005), reward monitoring (Hayden et al., 2008), emotional processing (Maddock et al., 2003) and mediation between task and rest states (Li et al., 2019; Utevsky et al., 2014). It also plays an important role in "default mode network" (DMN), functionally linked to self-consciousness (Cavanna and Trimble, 2006; Fransson and Marrelec, 2008), social cognitive functions (Mars et al., 2012), regulation of attentional states and cognition (Leech and Sharp, 2014; McKiernan et al., 2003), and which is known to appear later in the development of preterm infants (Smyser et al., 2010). Interestingly, resting-state functional MRI (rs-fMRI) has shown that the left PCUN plays a central role in integration in newborns and also belongs to the nodes hierarchically more important for the propagation of neural activity to other brain regions in FT but not in VPT infants, when at 10 years old (Padilla et al., 2020). Additionally, at TEA, rs-functional connectivity between the salience network and the PCUN has been shown to be significantly decreased in VPT-TEA infants in comparison to FT newborns (Lordier et al., 2019). Structural brain network studies have shown that the PCUN has an increased efficiency associated with longer gestational age when evaluated at preadolescent age (Kim et al., 2014), supporting the impact of prematurity in this node efficiency, and it presents a consistently high and increasing centrality from early infancy to adulthood (Chen et al., 2013; Hagmann et al., 2010; Huang et al., 2015). On the other hand, the superior temporal gyrus and the Heschl gyrus, which were detected as hubs in VPT-TEA but not in FT infants, have been shown to have a decreased centrality with age, from neonatal to preadolescence period (Huang et al., 2015). Such findings are thought to be related to a selective strengthening of the growing structural networks, through both microstructural enhancement of major WM tracts and axon pruning, based on a genetics and epigenetics background (Huang et al., 2015). Our results support the hypothesis of a delayed structural maturation in VPT-TEA structural brain networks, since the PCUN, a hub with increased centrality during development from term birth to adulthood, was found in FT newborns but not in VPT-TEA infants, while temporal regions that tend to have a decreased centrality during normal brain development were still identified as hubs in VPT-TEA, but not in FT infants. Another important reflection is that VPT infants are known to be exposed to many new different acoustic solicitations from the external world, in comparison to FT newborns that remain inside their mother's womb until term age. The differences in the acoustic environment might

lead to changes in activity-dependent synaptic plasticity and could justify the fact that temporal regions important for sound processing, such as the Heschl gyrus and the superior temporal gyrus (Fulford et al., 2004; Jardri et al., 2008), were found as hubs only in VPT-TEA infants.

Remarkably, VPT-TEA presented a superior number of hubs, with an inferior average number of connections, in comparison to FT newborns. This finding was confirmed and complemented by the reduced "rich-club" coefficient observed in VPT-TEA infants. A "rich-club" organization refers to the presence of some hub regions that are particularly densely connected to each other (more than what would be expected by chance) and is thought to be an important characteristic for efficient global information integration (van den Heuvel and Sporns, 2011; van den Heuvel et al., 2012). Literature has shown that the developmental window between 30 and 40 weeks GA, when preterm birth occurs, corresponds to an essential period for the establishment of connections between RC regions and the rest of the cortex, contributing to an increase in RC connectivity (Ball et al., 2014). Our data demonstrates, for the first time in literature, that VPT-TEA infants' structural brain networks have a higher number of hubs, but present a diminished weighted RC coefficient in comparison to FT infants, revealing thus a significantly diminished connectivity of highly connected and highly central brain regions in VPT-TEA vs FT infants, in agreement with our finding that in VPT-TEA brain networks are more segregated and less integrated than in FT infants. Ball et al. had found no difference between VPT-TEA and FT infants in the nodal degree within the RC domain, when considering only the connections among the RC nodes (Ball et al., 2014), but they have evaluated unweighted structural brain networks. Using fMRI, it has also been shown that VPT-TEA infants exhibit a significantly reduced functional connectivity within RC nodes in comparison to FT infants (Scheinost et al., 2016). Literature has also shown that longer gestation preferentially enhances RC connections and increases global network efficiency in the preadolescent brain (Kim et al., 2014). Additionally, an atypical RC organization has been found in various clinical disorders of neuronal connectivity, comprising attention-deficit/hyperactivity disorder (ADHD) and autism spectrum disorders (ASD), frequently observed in the preterm population (Ray et al., 2014). Our findings support thus not only the hypothesis that VPT-TEA infants' brain might present a delay in early development, with an organization which is typical of an earlier developmental stage in comparison to FT infants, but also that prematurity and its associated events might disrupt early structural connectivity and network organization.

4.2. Prematurity is associated with decreased connectivity strength in structural brain networks at TEA

In our study, VPT-TEA infants evidenced decreased connectivity strength in a set of inter and intra-hemispheric cortico-cortical connections, as well as in a set of intra-hemispheric cortico-subcortical and subcortico-subcortical connections in comparison to FT newborns. These findings are in agreement with other structural connectivity investigations in preterm infants (Ball et al., 2014; Bataille et al., 2017).

Among all cortical regions, the frontal cortex was the one exhibiting the majority of connections with decreased connectivity strength in VPT-TEA infants, with the OFC being the frontal region the most frequently involved. Decreased connectivity of the orbitofrontal network has already been shown in extremely preterm infants at 6 years of age (Fischi-Gomez et al., 2015). Literature has also shown that VPT infants present volumetric reductions, cortical immaturity and cortical gyrfication abnormalities in the OFC in comparison to FT infants (Ganella et al., 2015; Rogers et al., 2012; Thompson et al., 2007). These could be a consequence of the altered WM connectivity, to and from the OFC, that we find in VPT infants at TEA, and might be at the origin of the orbitofrontal specific cognitive and executive functioning deficits reported in preterm population (Luu et al., 2011; Mulder et al., 2009; Taylor and Clark, 2016).

From all the affected connections, the majority were intra-hemispheric cortico-cortical and, from these, the fronto-temporal connections were the most frequent, in particular those connecting the OFC to the TPO. These two regions were also the ones participating the most frequently in the connections with decreased connectivity strength in VPT-TEA. Both the OFC and the TPO have been considered as paralimbic regions, based on their anatomical location and connectivity (Duvernoy, 1999; Hof et al., 1995; Mesulam, 2000). One of the most important WM connections between the OFC and the TPO is the uncinate fasciculus (Oishi et al., 2015; Von Der Heide et al., 2013), which has been proven to be involved in behavioral and socio-emotional processing (Ghashghaei and Barbas, 2002; Kringelbach, 2005; Wildgruber et al., 2005) and to present a decreased maturation in prematurely born neonates, adolescents and adults (Constable et al., 2008; Mullen et al., 2011; Rimol et al., 2019; Sa de Almeida et al., 2019). After fronto-temporal connections, the fronto-limbic connections were the second most affected cortico-cortical connections. Indeed, these results are in agreement with previous studies, which have identified an immaturity of cortical fronto-temporal connectivity between VPT-TEA and FT infants (Pannek et al., 2013), as well as alterations in frontal-basal-ganglia-thalamocortical and limbic networks in 6 year-old infants born extremely prematurely, correlating with behavior and socio-emotional evaluation scores (Fischi-Gomez et al., 2016). Thus, our findings support the hypothesis that the diminished connectivity strength of frontal, paralimbic and limbic networks is already present in preterm infants by term-age and might be associated with the behavioral socio-emotional difficulties observed in prematurely born infants later in development (Bhutta et al., 2002; Fischi-Gomez et al., 2015; Hille et al., 2001; Hughes et al., 2002; Lejeune et al., 2015; Montagna and Nosarti, 2016; Spittle et al., 2009; Witt et al., 2014).

After the OFC and TPO, the PCG gyrus was the region the most frequently involved in the connections with decreased connectivity strength in VPT-TEA, as well as the most frequent among all limbic nodes participating in such connections. It was followed by the PCUN, which was also the most frequent among all parietal nodes participating in the connections with decreased connectivity strength in VPT-TEA infants. These two regions are part of DMN, which is associated with cognitive development (Palacios et al., 2013; Raichle et al., 2001) and is involved in a variety of high-level functions, such as attention and inhibitory control (Fair et al., 2008; Whitfield-Gabrieli and Ford, 2012), social cognition (Iacoboni et al., 2004), episodic memory (Greicius and Menon, 2004), and self-related processes (Gusnard et al., 2001). An altered DMN connectivity has been found to be associated with developmental disorders, such as ADHD (Castellanos et al., 2009; Fair et al., 2010) and ASD (Assaf et al., 2010; Nielsen et al., 2014), which are commonly reported in preterm population (Johnson and Marlow, 2011; Nosarti et al., 2012; Treyvaud et al., 2013). DMN is known to be incomplete/fragmented and with a posterior predominance in preterm infants, even at TEA, appearing later in their development (Doria et al., 2010; Fransson et al., 2007; Lordier et al., 2019; Smyser et al., 2010). Our results reveal that components from posterior DMN, namely the PCG and PCUN, have a decreased structural connectivity strength in VPT-TEA infants, in comparison to FT infants. This diminished structural connectivity might underlie the diminished functional connectivity observed in DMN in preterm infants at TEA and later in life (Lordier et al., 2019; Smyser et al., 2010; White et al., 2014), as well as the deficits in behavior and social cognition observed in this population (Anderson and Doyle, 2003; Arpi and Ferrari, 2013; Bhutta et al., 2002; Marlow, 2004; Montagna and Nosarti, 2016; Spittle et al., 2009; Witt et al., 2014).

Additionally, the left PCUN was the node the most frequently involved in inter-hemispheric connections with decreased connectivity strength in VPT-TEA infants, followed by the left DCG. Interestingly, these two regions were both detected as hubs in FT infants, evidencing thus a high centrality in this group, but not in VP-TEA infants. Inter-hemispheric connections are known to play an important role in long-range integration. The fact that the inter-hemispheric connections that

pass through the left PCUN and left DCG had a decreased connectivity strength in VPT-TEA infants, in comparison to FT infants, might explain why these two regions were detected as hubs only in FT infants, as well as the decreased integration capacity detected in VPT-TEA brain networks in comparison to FT infants.

4.3. Limitations and future directions

This study has limitations that have to be considered. First, the sample size is modest. This limitation is related to the difficulty of recruitment of newborns and families into a research project during a stressful time in their life, in particular for healthy FT newborns, where an MRI has only a limited clinical role. We are now recruiting a new cohort of VPT and FT infants for a second longitudinal study, which will allow to further validate our results. Second, although chi-squared test revealed no significant difference regarding the distribution of scanner/coils between groups, this is still a limitation to be taken into account. Furthermore, topup correction for EPI distortions was not applied in the present dataset, given the acquisition protocol. Such is a limitation that should be considered when interpreting the results from ACT tractography algorithm. Nevertheless, as we are comparing two groups of infants with the same age at MRI, the possible errors arriving from tractography would be similar between groups and thus data would be comparable. Additionally, we have opted to use SIFT for streamlines filtering, instead of the new available SIFT2 algorithm, mainly for the following reasons: 1) SIFT has been considered as effective in achieving its goal and has been used in previous recent neonatal connectome studies (Batalle et al., 2017; Blesa et al., 2019); 2) SIFT offers more flexibility in streamlines visualization; 3) SIFT allows more flexibility regarding subsequent analysis, since SIFT2 requires any following processing to be compatible with the definition of a cross-sectional multiplier for each streamline (Smith et al., 2015).

While our structural brain results support published data on specific neurocognitive and neurobehavioral deficits in preterm infants, the clinical significance of these specific brain structural alterations remains to be further evaluated by investigating neurodevelopmental and cognitive outcomes in this study population. These infants are currently being followed-up in our child development center with detailed neurodevelopmental assessments and the first results are expected within one year.

Given the specific alterations in network characteristics found in VPT infants at TEA, compared to FT infants, the question remains open as to the origin of these alterations. In our current longitudinal design, we are investigating if these brain network alterations are present in VPT infants already at birth or if they develop through the first weeks of life during NICU (neonatal intensive care unit) stay. This information will be crucial for the development of potential interventions aiming to prevent brain network alterations in preterm infants.

5. Conclusion

A whole-brain connectome analysis was used to study brain networks' differences between FT and VPT-TEA infants.

Overall, our results suggest that, although both FT and VPT-TEA groups evidence a small-world, modular and rich-club organization, VPT-TEA infants' brain networks display a typically more immature topology, compared to the expected development at term age. In particular, they evidence increased segregation and decreased integration, and thus a delayed shift from a local emphasis to a more distributed network architecture. The impaired integration might be explained by the detected increased modularity index, diminished rich-club coefficient and, in particular, by the observed decreased connectivity of typical neonatal hubs, such as bilateral thalamus, left PCUN and left DCG. Fronto-paralimbic and fronto-limbic were the most frequently affected connections in VPT-TEA. The noticeable decreased connectivity strength of the OFC-TPO circuitry might be at the origin of the behavior and socio-emotional difficulties associated with prematurity and thus early

interventions aiming to promote this circuitry plasticity might hold a relevant clinical impact in this population. Additionally, posterior regions from DMN, namely the PCUN and PCG, were also found to have a decreased structural connectivity in VPT-TEA infants, which might underlie the diminished functional connectivity of this network and thus the impaired behavioral and social cognition reported in preterm infants.

Declaration of Competing Interest

The authors declare no competing interests.

Credit authorship contribution statement

Joana Sa de Almeida: Formal analysis, Software, Methodology, Conceptualization, Writing - original draft. **Djalel-Eddine Meskaldji:** Validation, Writing - review & editing. **Serafeim Loukas:** Formal analysis, Writing - review & editing. **Lara Lordier:** Investigation, Writing - review & editing. **Laura Gui:** Formal analysis, Writing - review & editing. **François Lazeyras:** Resources, Investigation. **Petra S. Hüppi:** Conceptualization, Supervision, Project administration, Resources, Funding acquisition, Writing - review & editing.

Acknowledgments

The authors thank all clinical staff, namely in neonatology and unit of development of HUG Pediatric Hospital, all parents and newborns participating in the project, the Pediatrics Clinic Research Platform and the Center for Biomedical Imaging (CIBM) of the University Hospitals of Geneva, for all their valuable help and support.

Funding

This study was supported by grants from the [Swiss National Science Foundation](#) (n°32473B_135817/1 and n° 324730-163084), the Prim'enfance Foundation, the Swiss Government Excellence Scholarship, the Swiss Academy of Medical Sciences and the European Union's Horizon 2020 research and innovation programme under grant agreement [666992](#).

Supplementary materials

Supplementary material associated with this article can be found, in the online version, at [doi:10.1016/j.neuroimage.2020.117440](https://doi.org/10.1016/j.neuroimage.2020.117440).

References

- Alexander, G.E., Delong, M.R., Strick, P.L., 1986. Parallel organization of functionally segregated circuits linking basal ganglia and cortex. *Annu. Rev. Neurosci.* 9, 357–381. doi:[10.1146/annurev.ne.09.030186.002041](https://doi.org/10.1146/annurev.ne.09.030186.002041).
- Anderson, P., Doyle, L.W., 2003. Neurobehavioral outcomes of school-age children born extremely low birth weight or very preterm in the 1990s. *J. Am. Med. Assoc.* 289 (24), 3264–3272. doi:[10.1001/jama.289.24.3264](https://doi.org/10.1001/jama.289.24.3264).
- Andersson, J.L.R., Graham, M.S., Zsoldos, E., Sotiropoulos, S.N., 2016. Incorporating outlier detection and replacement into a non-parametric framework for movement and distortion correction of diffusion MR images. *NeuroImage* 141, 556–572. doi:[10.1016/j.neuroimage.2016.06.058](https://doi.org/10.1016/j.neuroimage.2016.06.058).
- Andersson, J.L.R., Sotiropoulos, S.N., 2016. An integrated approach to correction for off-resonance effects and subject movement in diffusion MR imaging. *NeuroImage* 125, 1063–1078. doi:[10.1016/j.neuroimage.2015.10.019](https://doi.org/10.1016/j.neuroimage.2015.10.019).
- Andersson, J.L.R., Graham, M.S., Drobjnjak, I., Zhang, H., Filippini, N., Bastiani, M., 2017. Towards a comprehensive framework for movement and distortion correction of diffusion MR images: within volume movement. *NeuroImage* 152, 450–466. doi:[10.1016/j.neuroimage.2017.02.085](https://doi.org/10.1016/j.neuroimage.2017.02.085).
- Anjari, M., Srinivasan, L., Allsop, J.M., Hajnal, J.V., Rutherford, M.A., Edwards, A.D., et al., 2007. Diffusion tensor imaging with tract-based spatial statistics reveals local white matter abnormalities in preterm infants. *NeuroImage* 35 (3), 1021–1027. doi:[10.1016/j.neuroimage.2007.01.035](https://doi.org/10.1016/j.neuroimage.2007.01.035).
- Arpi, E., Ferrari, F., 2013. Preterm birth and behaviour problems in infants and preschool-age children: a review of the recent literature. *Dev. Med. Child Neurol.* 55 (9), 788–796. doi:[10.1111/dmcn.12142](https://doi.org/10.1111/dmcn.12142).

- Assaf, M., Jagannathan, K., Calhoun, V.D., Miller, L., Stevens, M.C., Sahl, R., et al., 2010. Abnormal functional connectivity of default mode sub-networks in autism spectrum disorder patients. *NeuroImage* 53 (1), 247–256. doi:[10.1016/j.neuroimage.2010.05.067](https://doi.org/10.1016/j.neuroimage.2010.05.067).
- Avants, B.B., Tustison, N.J., Song, G., Cook, P.A., Klein, A., Gee, J.C., 2011. A reproducible evaluation of ANTs similarity metric performance in brain image registration. *NeuroImage* 54 (3), 2033–2044. doi:[10.1016/j.neuroimage.2010.09.025](https://doi.org/10.1016/j.neuroimage.2010.09.025).
- Ball, G., Boardman, J.P., Rueckert, D., Aljabar, P., Arichi, T., Merchant, N., et al., 2012. The effect of preterm birth on thalamic and cortical development. *Cereb Cortex* 22 (5), 1016–1024. doi:[10.1093/cercor/bhr176](https://doi.org/10.1093/cercor/bhr176).
- Ball, G., Boardman, J.P., Aljabar, P., Pandit, A., Arichi, T., Merchant, N., et al., 2013. The influence of preterm birth on the developing thalamocortical connectome. *Cortex; a journal devoted to the study of the nervous system and behavior* 49 (6), 1711–1721. doi:[10.1016/j.cortex.2012.07.006](https://doi.org/10.1016/j.cortex.2012.07.006).
- Ball, G., Aljabar, P., Zebari, S., Tusor, N., Arichi, T., Merchant, N., et al., 2014. Rich-club organization of the newborn human brain. *Proceedings of the National Academy of Sciences of the United States of America* 111 (20), 7456–7461. doi:[10.1073/pnas.1324118111](https://doi.org/10.1073/pnas.1324118111).
- Ball, G., Pazderova, L., Chew, A., Tusor, N., Merchant, N., Arichi, T., et al., 2015. Thalamocortical Connectivity Predicts Cognition in Children Born Preterm. *Cerebral Cortex* 25 (11), 4310–4318. doi:[10.1093/cercor/bhu331](https://doi.org/10.1093/cercor/bhu331).
- Ball, G., Aljabar, P., Nongena, P., Kennea, N., Gonzalez-Cinca, N., Falconer, S., et al., 2017. Multimodal image analysis of clinical influences on preterm brain development. *Ann Neurol* 82 (2), 233–246. doi:[10.1002/ana.24995](https://doi.org/10.1002/ana.24995).
- Bassett, D.S., Wymbs, N.F., Porter, M.A., Mucha, P.J., Carlson, J.M., Grafton, S.T., 2011. Dynamic reconfiguration of human brain networks during learning. *Proc. Natl. Acad. Sci. U.S.A.* 108 (18), 7641–7646. doi:[10.1073/pnas.1018985108](https://doi.org/10.1073/pnas.1018985108).
- Bassett, D.S., Yang, M., Wymbs, N.F., Grafton, S.T., 2015. Learning-induced autonomy of sensorimotor systems. *Nat Neurosci* 18 (5), 744–751. doi:[10.1038/nn.3993](https://doi.org/10.1038/nn.3993).
- Bastiani, M., Andersson, J.L.R., Cordero-Grande, L., Murgasova, M., Hutter, J., Price, A.N., et al., 2019. Automated processing pipeline for neonatal diffusion MRI in the developing Human Connectome Project. *NeuroImage* 185, 750–763. doi:[10.1016/j.neuroimage.2018.05.064](https://doi.org/10.1016/j.neuroimage.2018.05.064).
- Batalle, D., Hughes, E.J., Zhang, H., Tournier, J.D., Tusor, N., Aljabar, P., et al., 2017. Early development of structural networks and the impact of prematurity on brain connectivity. *NeuroImage* 149, 379–392. doi:[10.1016/j.neuroimage.2017.01.065](https://doi.org/10.1016/j.neuroimage.2017.01.065).
- Behrens, T.E.J., Woolrich, M.W., Jenkinson, M., Johansen-Berg, H., Nunes, R.G., Clare, S., et al., 2003. Characterization and propagation of uncertainty in diffusion-weighted MR imaging. *Magn. Reson. Med.* 50 (5), 1077–1088. doi:[10.1002/mrm.10609](https://doi.org/10.1002/mrm.10609).
- Benjamini, Y., Hochberg, Y., 1995. Controlling the False Discovery Rate - a Practical and Powerful Approach to Multiple Testing. *J. R. Stat. Soc. Ser. B Stat. Methodol.* 57 (1), 289–300. doi:[10.1111/j.2517-6161.1995.tb02031.x](https://doi.org/10.1111/j.2517-6161.1995.tb02031.x).
- Bhutta, A.T., Cleves, M.A., Casey, P.H., Cradock, M.M., Anand, K.J.S., 2002. Cognitive and behavioral outcomes of school-aged children who were born preterm - A meta-analysis. *J. Am. Med. Assoc.* 288 (6), 728–737. doi:[10.1001/jama.288.6.728](https://doi.org/10.1001/jama.288.6.728).
- Blesa, M., Sullivan, G., Anblagan, D., Telford, E.J., Quigley, A.J., Sparrow, S.A., et al., 2019. Early breast milk exposure modifies brain connectivity in preterm infants. *NeuroImage* 184, 431–439. doi:[10.1016/j.neuroimage.2018.09.045](https://doi.org/10.1016/j.neuroimage.2018.09.045).
- Bressler, S.L., 1995. Large-Scale Cortical Networks and Cognition. *Brain Res. Rev.* 20 (3), 288–304. doi:[10.1016/0165-0173\(94\)00016-I](https://doi.org/10.1016/0165-0173(94)00016-I), doi:Doi.
- Bressler, S.L., Menon, V., 2010. Large-scale brain networks in cognition: emerging methods and principles. *Trends cogn. sci.* 14 (6), 277–290. doi:[10.1016/j.tics.2010.04.004](https://doi.org/10.1016/j.tics.2010.04.004).
- Brown, C.J., Miller, S.P., Booth, B.G., Andrews, S., Chau, V., Poskitt, K.J., et al., 2014. Structural network analysis of brain development in young preterm neonates. *NeuroImage* 101, 667–680. doi:[10.1016/j.neuroimage.2014.07.030](https://doi.org/10.1016/j.neuroimage.2014.07.030).
- Bullmore, E.T., Sporns, O., 2009. Complex brain networks: graph theoretical analysis of structural and functional systems. *Nat. Rev. Neurosci.* 10 (3), 186–198. doi:[10.1038/nrn2575](https://doi.org/10.1038/nrn2575).
- Castellanos, F.X., Kelly, C., Milham, M.P., 2009. The Restless Brain: Attention-Deficit Hyperactivity Disorder, Resting-State Functional Connectivity, and Intrasubject Variability. *Canadian Journal of Psychiatry-Revue Canadienne De Psychiatrie* 54 (10), 665–672. doi:[10.1177/070674370905401003](https://doi.org/10.1177/070674370905401003).
- Cavanna, A.E., Trimble, M.R., 2006. The precuneus: a review of its functional anatomy and behavioural correlates. *Brain* 129, 564–583. doi:[10.1093/brain/awl004](https://doi.org/10.1093/brain/awl004).
- Chen, Z., Liu, M., Gross, D.W., Beaulieu, C., 2013. Graph theoretical analysis of developmental patterns of the white matter network. *Front. Hum. Neurosci.* 7, 716. doi:[10.3389/fnhum.2013.00716](https://doi.org/10.3389/fnhum.2013.00716).
- Cismaru, A.L., Gui, L., Vasung, L., Lejeune, F., Barisnikov, K., Truttmann, A., et al., 2016. Altered Amygdala Development and Fear Processing in Prematurely Born Infants. *Front. Neuroanat.* 10, 55. doi:[10.3389/fnana.2016.00055](https://doi.org/10.3389/fnana.2016.00055).
- Constable, R.T., Ment, L.R., Vohr, B.R., Kesler, S.R., Fulbright, R.K., Lacadie, C., et al., 2008. Prematurely born children demonstrate white matter microstructural differences at 12 years of age, relative to term control subjects: An investigation of group and gender effects. *Pediatrics* 121 (2), 306–316. doi:[10.1542/peds.2007-0414](https://doi.org/10.1542/peds.2007-0414).
- Crossley, N.A., Mechelli, A., Scott, J., Carletti, F., Fox, P.T., McGuire, P., et al., 2015. The hubs of the human connectome are generally implicated in the anatomy of brain disorders. *Brain* 137 (Pt 8), 2382–2395. doi:[10.1093/brain/awu132](https://doi.org/10.1093/brain/awu132).
- Doria, V., Beckmann, C.F., Arichi, T., Merchant, N., Groppo, M., Turkheimer, F.E., et al., 2010. Emergence of resting state networks in the preterm human brain. *Proc. Natl. Acad. Sci. U.S.A.* 107 (46), 20015–20020. doi:[10.1073/pnas.1007921107](https://doi.org/10.1073/pnas.1007921107).
- Dubois, J., Dehaene-Lambertz, G., Perrin, M., Mangin, J.-F., Cointepas, Y., Duchesnay, E., et al., 2008. Asynchrony of the early maturation of white matter bundles in healthy infants: quantitative landmarks revealed noninvasively by diffusion tensor imaging. *Hum. Brain Mapp.* 29 (1), 14–27. doi:[10.1002/hbm.20363](https://doi.org/10.1002/hbm.20363).
- Duvernoy, H.M., 1999. *The human brain. Surface, blood supply, and three-dimensional sectional anatomy.* Springer Wien, New York.

- in Schizophrenia. *JAMA Psychiatry* 70 (8), 783–792. doi:[10.1001/jamapsychiatry.2013.1328](https://doi.org/10.1001/jamapsychiatry.2013.1328).
- Von Der Heide, R.J., Skipper, L.M., Klobusicky, E., Olson, I.R., 2013. Dissecting the uncinate fasciculus: disorders, controversies and a hypothesis. *Brain* 136, 1692–1707. doi:[10.1093/brain/awt094](https://doi.org/10.1093/brain/awt094).
- Watts, D.J., Strogatz, S.H., 1998. Collective dynamics of 'small-world' networks. *Nature* 393 (6684), 440–442. doi:[10.1038/30918](https://doi.org/10.1038/30918).
- Wee, C.Y., Tuan, T.A., Broekman, B.F.P., Ong, M.Y., Chong, Y.S., Kwek, K., et al., 2017. Neonatal Neural Networks Predict Children Behavioral Profiles Later in Life. *Hum. Brain Mapp.* 38 (3), 1362–1373. doi:[10.1002/hbm.23459](https://doi.org/10.1002/hbm.23459).
- White, T.P., Symington, I., Castellanos, N.P., Brittain, P.J., Walsh, S.F., Nam, K.W., et al., 2014. Dysconnectivity of neurocognitive networks at rest in very-preterm born adults. *NeuroImage-Clinical* 4, 352–365. doi:[10.1016/j.nicl.2014.01.005](https://doi.org/10.1016/j.nicl.2014.01.005).
- Whitfield-Gabrieli, S., Ford, J.M., 2012. Default Mode Network Activity and Connectivity in Psychopathology. *Annual Review of Clinical Psychology* 8. doi:[10.1146/annurev-clinpsy-032511-143049](https://doi.org/10.1146/annurev-clinpsy-032511-143049), 49–+.
- Wildgruber, D., Riecker, A., Hertrich, I., Erb, M., Grodd, W., Ethofer, T., et al., 2005. Identification of emotional intonation evaluated by fMRI. *NeuroImage* 24 (4), 1233–1241. doi:[10.1016/j.neuroimage.2004.10.034](https://doi.org/10.1016/j.neuroimage.2004.10.034).
- Witt, A., Theurel, A., Tolsa, C.B., Lejeune, F., Fernandes, L., de Jonge, L., et al., 2014. Emotional and effortful control abilities in 42-month-old very preterm and full-term children. *Early Hum Dev* 90 (10), 565–569. doi:[10.1016/j.earlhumdev.2014.07.008](https://doi.org/10.1016/j.earlhumdev.2014.07.008).
- Yap, P.T., Fan, Y., Chen, Y.S., Gilmore, J.H., Lin, W.L., Shen, D.G., 2011. Development Trends of White Matter Connectivity in the First Years of Life. *PLoS ONE* 6 (9), e24678. doi:[10.1371/journal.pone.0024678](https://doi.org/10.1371/journal.pone.0024678).
- Zalesky, A., Fornito, A., Bullmore, E.T., 2010. Network-based statistic: Identifying differences in brain networks. *NeuroImage* 53 (4), 1197–1207. doi:[10.1016/j.neuroimage.2010.06.041](https://doi.org/10.1016/j.neuroimage.2010.06.041).
- Zhao, T.D., Mishra, V., Jeon, T., Ouyang, M.H., Peng, Q.M., Chalak, L., et al., 2019. Structural network maturation of the preterm human brain. *NeuroImage* 185, 699–710. doi:[10.1016/j.neuroimage.2018.06.047](https://doi.org/10.1016/j.neuroimage.2018.06.047).